

Updates to the AMUR code for R-matrix analyses on heavy nuclei

Satoshi Kunieda^{1,*}, Shunsuke Endo^{1,**}, and Atsushi Kimura^{1,***}

¹Japan Atomic Energy Agency, Shirakata 2-4, Tokai-mura, Ibaraki 319-1195, Japan

Abstract. The AMUR code, that had been initially designed for R-matrix analysis on light nuclei, was updated to perform resonance analyses on heavy nuclei by including approximated theories with experimental corrections such as resolution function. As a feasibility study, we tested these updates by performing a covariance analysis on J-PARC/ANNRI measured data for n+⁹³Nb reactions. In this work we present preliminary results obtained from the fitting procedure including both R-matrix resonance parameters and parameters related to the experimental corrections. We also discuss about physical constraint from the theory for forthcoming in-depth analysis to the measurements.

1 Introduction

The AMUR code [1, 2], which is based on the R-matrix nuclear reaction theory [3] and the Kalman filtering method [4] for the data-assimilation, is under development in JAEA for the cross-section evaluation with the covariance data in the resolved resonance energy region. The code was initially designed for the analysis of the light-nuclei to narrow large differences of cross-sections among evaluations in the world (e.g., on n+¹⁶O [1]). Also, it was applied to the development of JENDL-5 [5] for a number of light-mass isotopes such as ^{12,13}C, ¹⁵N, ¹⁶O and ¹⁹F. Recently, the authors extended capability of the code toward the analysis of heavier nuclei by introducing the Reich-Moore approximation [6] to calculate the radiative-capture and fission cross-sections. The code is also able to calculate the Doppler broadening with the free-gas approximation. In addition to those capabilities, we understand that in-depth resonance analysis requires a number of corrections which depend on the experimental conditions.

In this work, we challenge a resonance analysis of neutron cross-section data measured in J-PARC/ANNRI [7] with AMUR. The self-shielding and multiple-scattering effects in the target sample should be considered in the resonance analysis, however, the implementation of such correction into the code is under investigation. Therefore, the experimental data to be analyzed in this study are those corrected by the Monte Carlo simulation. Under this precondition, fundamental challenge on the analysis may be consideration of the energy resolution for incident neutrons with the double-bunching problem in the time-of-flight (TOF) measurements at our accelerator facility. In this study, we incorporate the resolution functions estimated by Kino et al. [8] into the code to take account such experimental conditions in the resonance analysis. We de-

vote our much efforts to a feasibility study of the covariance/uncertainty analysis on the J-PARC/ANNRI measurements, where a test analysis was demonstrated on the ⁹³Nb isotope. Preliminary results of fitting parameters and cross-sections are also presented. Finally, let us discuss about physical constraints from the R-matrix theory (constraints from behavior of the phase-shifts and the interference effects) for forthcoming in-depth/sophisticated analysis to the measurements.

2 Extension on AMUR toward analysis of heavier nuclei

2.1 Basic capabilities on theoretical calculation

AMUR was initially developed for the analysis of the light-nuclei to narrow large differences of cross-sections among evaluations in the world, e.g., on the ¹⁶O(n,α) cross-section, by making used of the theoretical constraints [1] from the R-matrix theory. The code was also designed to analyze covariance data of the resonance parameters and cross-sections, where both the experimental and theoretical knowledge were reflected to the nuclear data evaluation as much as possible [2]. The analysis on the heavier nuclei is different from that for the light nuclei in general as follows.

- A great number of levels should be analyzed, although the number of channel spin is limited.
- The fission reaction should be included for the actinide nuclei.
- It is much important to take account of the experimental conditions.

We thought that AMUR could be applied to analysis on the heavier nuclei if the code is updated for those differences, learning a number of experiences on the other codes such as SAMMY [9] and REFIT [10].

*e-mail: kunieda.satoshi@jaea.go.jp

**e-mail: endo.shunsuke@jaea.go.jp

***e-mail: kimura.atsushi@jaea.go.jp

Recently, the authors extended capabilities of the code toward the analysis of medium- and heavy-mass nuclei to fully cover range of isotopes required for nuclear science and engineering. In the theoretical part, AMUR is now able to read resonance parameter set stored in the ENDF-6 format (MF=2) files, then performs reconstruction with the Breit-Wigner (LRF=1,2) or the Reich-Moore type formulae (LRF=3,7), which means the code is able to calculate radiative capture and fission cross-sections with approximated/reduced R-matrix formulae. The code is also able to perform the Doppler broadening with the free-gas approximation. Once the areal density of sample material is given, the transmission is calculated from the total cross-sections. Figure 1 illustrates neutron transmission on ^{233}U measured by Guber *et al.* [11] and calculated results of AMUR with resonance parameter set (LRF=3) in ENDF/B-VIII.0 [12]. We have not yet made thorough comparisons with other codes, this figure visually suggests AMUR is getting equivalent with the other resonance analysis codes in terms of basic capabilities for calculating/reconstructing the cross-sections.

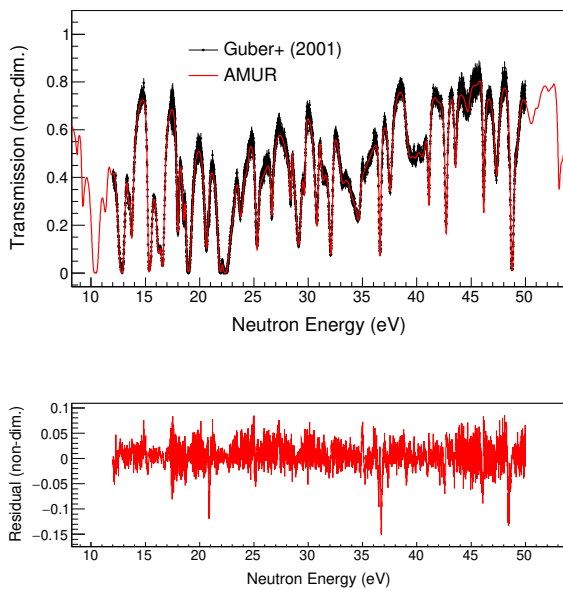


Figure 1. Neutron transmission on ^{233}U measured by Guber *et al.* [11] and calculated results of AMUR with resonance parameter set (LRF=3) in ENDF/B-VIII.0 [12] where the residuals are plotted in the bottom panel.

2.2 Resolution function

In general, experimental data are different from true values of the cross-sections, because the data are measured under intrinsic experimental conditions such as on the accelerator facility, detection system, composition of the sample, and so forth. Therefore, it is necessary to simulate such experimental conditions as much as possible in the resonance analysis or the nuclear data evaluation. In this regard, time/energy structure of the incident neutrons

is one of the most important factors in the cross-sections measurements.

The cross-section measurements are underway in the J-PARC/MLF facility with the TOF method and the AN-NRI detection system to measure neutron cross-sections for minor actinides and structural material in the resolved resonance energy region. The facility shows its own time structure of neutron beam, where the operation of the proton accelerator is usually in the double-bunch mode, which eventually results in degeneration of resonant structure on the cross-sections.

The resolution function of J-PARC/MLF had been estimated by Kino *et al.* [8]. The study had been based on the Monte Carlo simulation that was validated by a number of experimental campaigns at the same facility. The function had already been applied to the resonance analysis code REFIT [10, 13], which enabled us to have a number of experiences on the resonance analysis (The most recent work is found in Ref. [14]). Recently, those works were followed by one of the authors and the function was incorporated into AMUR. Figure 2 illustrates 2D plots of the calculated resolution functions in the single- and double-bunch modes. With the AMUR code, energy distribution of the incident neutrons are calculated at an arbitrary flight time. The figure shows that we successfully followed the work of Kino *et al.* [8] where significance of the double-bunching effect is seen above 10 eV of the incident neutrons.

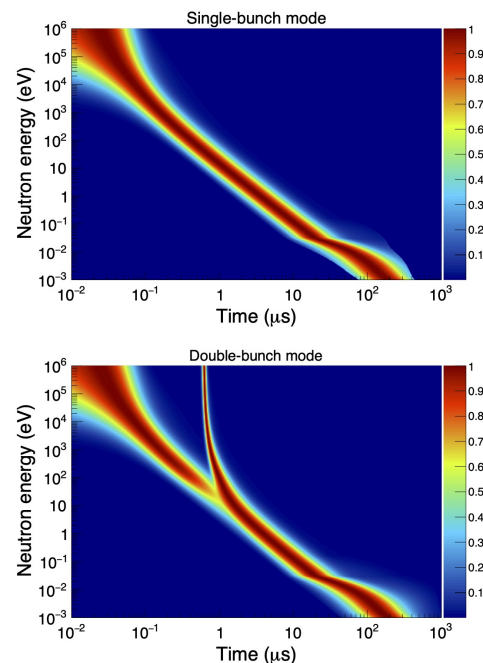


Figure 2. Resolution functions of the J-PARC/MLF facility in the single- and double-bunch modes calculated by the AMUR code base on the work of Kino *et al.* [8]

In this work, the code was eventually updated to analyze TOF measurements directly. For example, values of the time-dependent neutron transmission which are to be compared with experimental data are calculated by the

equations as follows,

$$T_{rans}(t) = \int_0^{\infty} R(L, t + t_0, E) T_{rans}(E) dE, \quad (1)$$

where the symbol $R(L, t + t_0, E)$ denotes the resolution function that also depends on the flight path L and initial delay t_0 in the measurements. The energy dependent transmission $T_{rans}(E)$ is calculated with target thickness n , composition of i -th isotope in the sample c_i and the total cross-section $\sigma_i(E, T)$ reconstructed at temperature T :

$$T_{rans}(E) = \exp\left(-n \sum_i c_i \times \sigma_i(E, T)\right). \quad (2)$$

3 Preliminary analysis of J-PARC/ANNRI measurements

3.1 Experimental data to be analyzed

Quite recently, some of the authors measured transmission and (n, γ) cross-sections on ^{93}Nb [14] at J-PARC/MLF. This measurement is one of the good practices for the updated version of AMUR because of reasons as follows.

- ^{93}Nb is a mono isotope in which possible effects from the other isotopes are expected to be minimized.
- In the experimental campaign, both the transmission and (n, γ) cross-sections are measured, which allows us to obtain values of the resonance parameters both for neutron and γ -ray reaction channels, consistently.
- The experiments had been performed in the double-bunch mode of accelerator. That is a good practice for AMUR with new option of the resolution function.

In this study, we analyze those experimental data up to 400 eV, in which both the theoretical and experimental parameters are searched for, simultaneously.

3.2 Prior parameters and covariances

Among a number of the approximated resonance formulae which are stemmed from the R-matrix theory, we adopted the Reich-Moore type (ENDF-6/MF=2/LRF=3) to calculate/reconstruct the cross-sections, as a first step of AMUR being applied to heavier nuclei. Initial of the resonance parameter set was taken from the preceding work by Endo *et al.* [14] in which parameter values had been obtained from the same measurements with the modified REFIT code that accommodates to the double-bunching issue.

In the analysis, based on our experiences, prior uncertainty values were assumed 1 eV for the resonance energies E_r and 10% for neutron and radiation widths, Γ_n and Γ_γ . With those prior parameters, the calculated total cross-section and its correlations matrix are shown in Fig. 3, where energy grid in both plots are obtained so as to retain accuracy of 0.1% for the interpolation. The matrix is very complicated, showing both the short- and long-range correlation due to the interference between/among

the resonances and the non-resonant processes. Furthermore, value of correlation is suddenly minimized at the peak positions because phase-shifts of the elastic scattering process should be maximized toward $\pi/2$ at the resonant energies. Those correlations are visually suggesting that physical constraints certainly exist in analysis of experimental data. Thus, it is interesting to see how such theoretical constraints are showing up in the resonance analysis, which will be discussed in the next subsection/section.

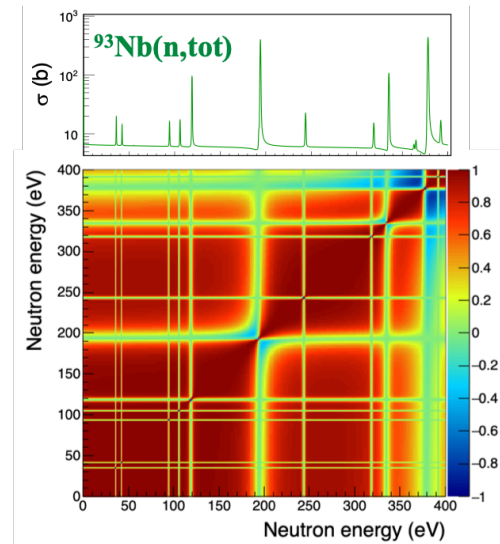


Figure 3. Calculate total cross-section and its correlation matrix on ^{93}Nb with prior parameters and uncertainties described in the texts.

In the present analysis, learning a number of experiences with the SAMMY and REFIT codes, we also introduced the experimental parameters to be searched for. Those parameters preliminary assumed were the flight-path and initial delay of the TOF measurements. The sample thickness/normalization and amount of contaminant isotope (only ^{181}Ta was assumed in this test case) were also treated as free parameters. Although their values could be quantified by measurements, the accuracy is sometimes questionable, which may results in one of the large causes of uncertainty on the evaluated cross-sections. We expected that such experimental parameters could be obtained through resonance analysis because the theory may impose constraints not only on the values of resonance parameters but also on behaviors of the experimental parameters.

3.3 Fitting results

All the resonance parameters and a limited number of the experimental parameters listed in Table 1 were simultaneously searched for, by fitting the experimental data of the ^{93}Nb isotope measured at J-PARC with the updated version of AMUR described in Sec. 2. Figure 4 illustrates fitting results to TOF spectra on the transmission and (n, γ) cross-section measurements. The fitting itself was nearly

perfect as we successfully reproduced experimental data, in which the double-bunching and a contaminant (^{181}Ta) effect was simulated well.

Transmission		
Parameter	Prior	Posterior
Flight path (m)	28.68 (1%)	28.674 (0.001%)
Initial delay (us)	3.50 (1%)	3.528 (0.069%)
Thickness (atoms/b)	0.01673 (3%)	0.01408 (0.559%)

(n,γ)		
Parameter	Prior	Posterior
Flight path (m)	21.52 (1%)	21.490 (0.003%)
Initial delay (us)	4.1 (1%)	4.230 (0.072%)
Normalization to calc.	1.00 (10%)	0.916 (1.01%)
Ta-181/Nb-93	0.0006 (3%)	0.00064 (1.10%)

Table 1. The experimental parameter values and their uncertainties obtained in the present analysis.

The experimental parameter values obtained are listed in Table 1 together with their uncertainties, in which the prior and posterior values are compared for a reference purpose. The flight-path and initial delay were determined within uncertainties less than 0.1% and they were very close to the prior values obtained by the measurement. It is noticeable that the resulting values of the sample thickness/normalization were estimated with uncertainties of $\lesssim 1\%$, but the nominal values are different from the priors by $\sim 10\%$. This time, let us avoid in-depth discussion on such values and the differences because we understand that there could be the other sources in the experimental condition. However, our preliminary result suggests that the theoretical constraint is so large that the resonance analysis allows us to quantify experimental parameters which are difficult to know only by the measurement. For instance, it is virtually impossible to eliminate the systematic uncertainty from the experimental data in general, where the present approach may give us a useful guide to tackle this problem.

4 Resulting covariances

The covariances of the parameter values were obtained through the fitting procedure. Once we calculate sensitivities of the parameters to the cross-sections, covariance matrices of cross-sections are estimated by the propagation law. The resulting correlation matrices are illustrated in Fig. 5 for total and (n,γ) cross-sections. In respect to analysis of the J-PARC/ANNRI measurements, we are now presenting such correlations of cross-sections for the first time. It is an advantageous feature of AMUR to immediately calculate and visualize correlations with a parallel processing technique.

We firstly see overall features of those plots are quite complicated because of the interference effects on the resonant nuclear reaction. Nevertheless, it is interesting to see the correlation values are drastically minimized/maximized at resonance positions. That is a consequence of quantum mechanical physics in the resonant

reaction where the phase-shifts are maximized at the peak position as touched on Sec. 3.2. A strong long-range correlation is seen in the total cross-sections. Since such a trend is not observed in the (n,γ) reaction, such a long-range correlation comes from the elastic scattering. It is true that the shape elastic scattering process, which is calculated by the hard-sphere model in R-matrix, always occurs over the energy range. Medium-range correlations observed in the (n,γ) reaction are due to a number of reasons. For instance, a strong correlation that appears below 100 eV is mainly due to negative levels which exist below neutron separation energy of the compound nuclei. The tails of large resonances produce the other strong correlations observed in higher energy region. Furthermore, the experimental parameters (such as normalization parameter) should be sources of the long-range correlation, as we did see correlations between the resonance and experimental parameters. We believe that it is valuable to see correlation matrices of cross-sections in this way, because they show us physical features of the resonant reactions which could be one of the bases of an elaborate analysis to the experimental data.

Figure 6 illustrates resulting $^{93}\text{Nb}(n,\gamma)$ cross-sections and their uncertainty values. The uncertainty we obtained was $\sim 5\%$ on average but highly depend on neutron energy or structure of resonances. The fact may be because of the R-matrix theory in which the physical constraint is maximized at peak positions of the resonances. We are not yet fully understood physical background of resulting uncertainty. Nevertheless, that may give a reasonable uncertain of cross-sections since the present analysis is based on knowledges both on the experiment and theory.

5 Summary

The AMUR code was updated for analysis of cross-sections on heavier nuclei in terms of both the theoretical calculation and the experimental correction. In the theoretical part, resonance formulae used in the ENDF-6 format (MF=2/LRF=1,2,3 and 7) were incorporated to the code together with a capability of the Doppler broadening. In the experimental part, we devoted our much efforts to simulation of the resolution function in the J-PARC/ANNRI measurements. Those options were applied to the resonance analysis of ^{93}Nb , and we found the fitting itself was quite successful in which both resonance and experimental parameters obtained were expected to be reasonable.

In this work, we derived correlation matrices of cross-sections with AMUR for the same isotope. It was first time to perform covariance analysis of cross-sections based on the J-PARC/ANNRI measurement. The resulting correlation matrices were complicated to be fully understood but we certainly saw traces of physical constraints from the R-matrix theory. The same discussion could be possible for the uncertainty of cross-sections obtained in this analysis. This time, let us conclude that we successfully obtained theoretical and experimental parameters with covariance/correlation matrices with AMUR despite the double-bunching problem of the facility. In-depth analysis

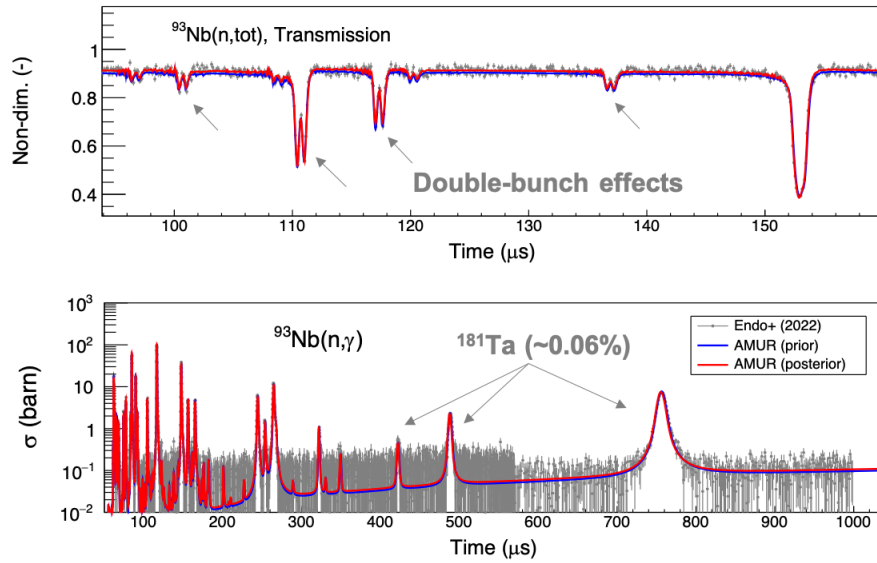


Figure 4. Fitting results to the experimental TOF spectra on transmission and (n,γ) cross-sections measured at J-PARC/ANNRI.

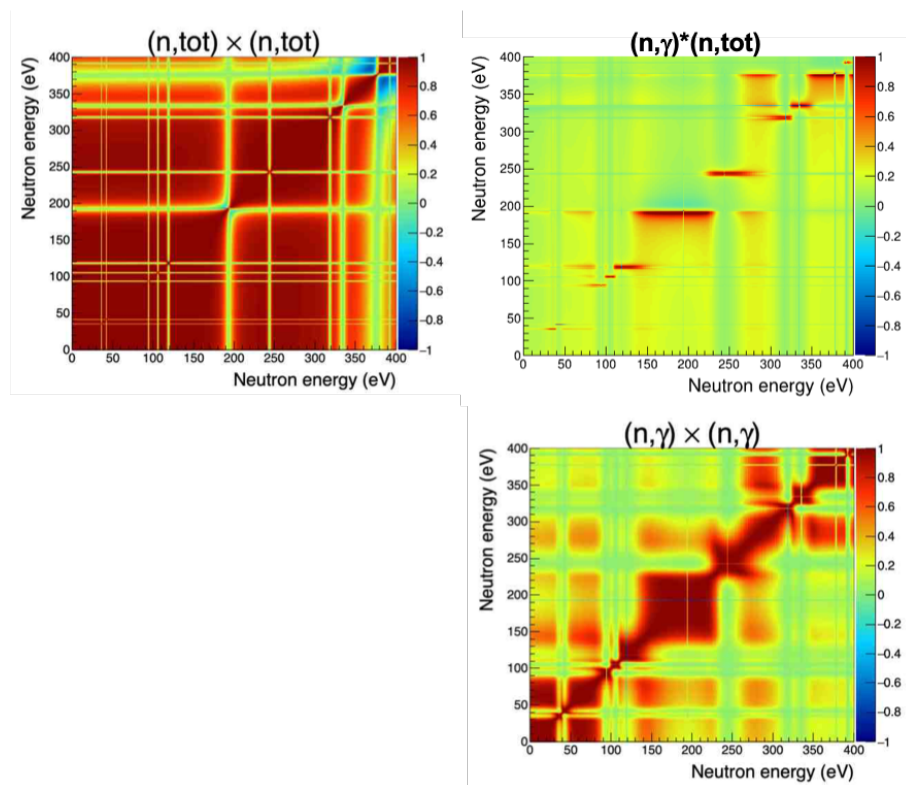


Figure 5. Correlation matrices for $n+^{93}\text{Nb}$ total and (n,γ) cross sections.

is to be continued both from the experimental and theoretical points of views.

References

- [1] S. Kunieda, T. Kawano, M. Paris, et al., Nucl. Data Sheets **118**, 250 (2014)
- [2] S. Kunieda, T. Kawano, M. Paris, et al., Nucl. Data Sheets **123**, 159 (2015)
- [3] A.M. Lane, R.G. Thomas, Rev. Mod. Phys. **30**, 257 (1958)
- [4] T. Kawano, H. Matsunobu, T. Murata, et al., J. Nucl. Sci. Technol. (Tokyo) **37**, 327 (2000)
- [5] O. Iwamoto, N. Iwamoto, S. Kunieda, et al, J. Nucl. Sci. Technol. **60(1)**, 1 (2023)
- [6] C.W. Reich, M.S. Moore, Phys. Rev. **111**, 929 (1958)

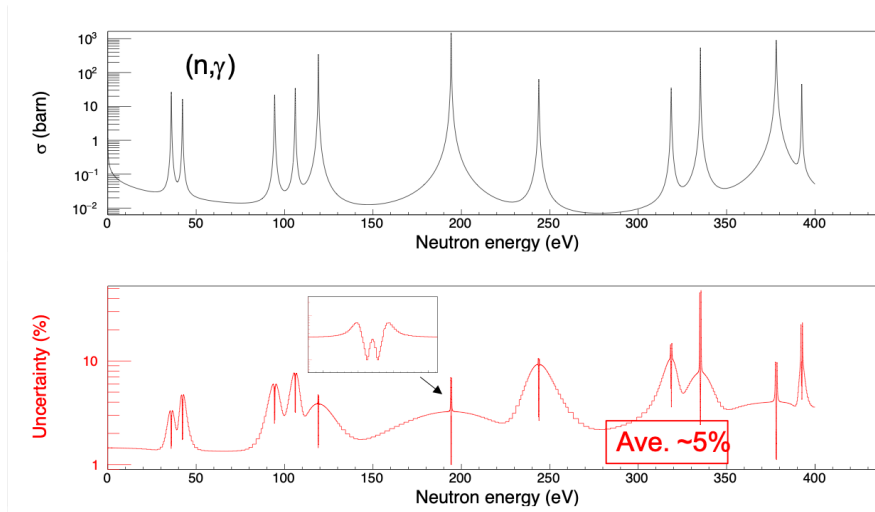


Figure 6. $^{93}\text{Nb}(n,\gamma)$ cross section (top) and corresponding relative uncertainty in percent (bottom).

- [7] M. Igashira, Y. Kiyonagi, M. Oshima, Nuclear Instruments and Methods in Physics Research Section A: Accelerators Spectrometers, Detectors and Associated Equipment **600**, 332 (2009)
- [8] K. Kino, M. Furusaka, F. Hiraga, et al., Nuclear Instruments and Methods in Physics Research Section A: Accelerators, Spectrometers, Detectors and Associated Equipment **736**, 66 (2014)
- [9] M.N. Larson, Updated user's guide for SAMMY: mul-tilevel R-matrix fits to neutron data using Bayes' equations, ORNL/TM-9179/R4. Oak Ridge National Laboratory; 1998.
- [10] M.C. Moxon, T.C. Ware, C.J. Dean, Users' guide for REFIT-2009-10, UKNSF; 2010 April. pp. 243. UK Nuclear Science Forum
- [11] K.H. Guber, R.R. Spencer, L.C. Leal, P.E. Koehler, J.A. Harvey, R.O. Sayer, H. Derrien, T.E. Valentine, D.E. Pierce, V.M. Cauley et al., Nuclear Science and Engineering **139**, 111 (2001)
- [12] D.A. Brown, M.B. Chadwick, R. Capote, A.C. Kahler, A. Trkov, M.W. Herman, A.A. Sonzogni, Y. Danon, A.D. Carlson, M. Dunn et al., Nuclear Data Sheets **148**, 1 (2018), special Issue on Nuclear Reaction Data
- [13] H. Hasemi, M. Harada, T. Kai, et al., Nuclear Instruments and Methods in Physics Research Section A: Accelerators, Spectrometers, Detectors and Associated Equipment **773**, 137 (2015)
- [14] S. Endo, A. Kimura, S. Nakamura, et al., Journal of Nuclear Science and Technology **59**, 318 (2022)